



Short communication

New trivalent imidazole-derived salt for lithium-ion cell electrolyte



Tomasz Trzeciak^a, Leszek Niedzicki^{a,*}, Grazyna Groszek^b, Piotr Wieczorek^a,
Marek Marcinek^a, Wladyslaw Wieczorek^a

^a Faculty of Chemistry, Warsaw University of Technology, Noakowskiego 3, 00664 Warsaw, Poland

^b Faculty of Chemistry, Rzeszow University of Technology, Powstancow Warszawy 6, 35959 Rzeszow, Poland

HIGHLIGHTS

- First trivalent lithium non-sulfonyl salt for Li-ion cells was synthesized.
- New Li₃BTI salt is stable thermally and electrochemically.
- Ionic conductivity in battery solvent mixture (EC:DMC) and in PC is investigated.
- Electrolytes with Li₃BTI have high lithium cation transference number (above 0.7).
- Cycling in half-cell shows very good electrolyte stability behavior.

ARTICLE INFO

Article history:

Received 22 August 2013

Received in revised form

28 November 2013

Accepted 3 December 2013

Available online 14 December 2013

Keywords:

Lithium-ion

Salt

Multivalent

Electrolyte

Synthesis

Imidazole

ABSTRACT

Lithium-ion cells utilize almost exclusively monovalent lithium salts as main electrolyte component. Apart from scarce works on sulfonyl imide derivatives, even in terms of basic parameters little is known about multivalent lithium salts' behavior in electrolytes. Here we present the new trivalent lithium salt dedicated to electrolytes for lithium-ion cells. Trilithium 2,2',2''-tris(trifluoromethyl)benzotris(imidazolate) (Li₃BTI) synthesis and its performance in PC and EC:DMC solutions is described in this paper. The structure and stability of this new lithium salt was fully characterized by NMR and Raman techniques as well as thermal methods. Basic electrochemical parameters of electrolytes based on this salt were done by linear sweep voltammetry, lithium cation transference number and conductivity measurements. The salt was designed specifically to manifest extraordinarily high lithium cation transference number (0.73 in EC:DMC 1:1 ratio mixture). However this new salt exhibits also thermal stability of 160 °C and electrochemical stability up to 4.5 V vs Li, as well as conductivities of the 1 mS cm⁻¹ order of magnitude in liquid electrolytes. Promising compatibility results of the obtained electrolyte against Si/C composite anodes are also reported in this paper.

© 2013 Elsevier B.V. All rights reserved.

1. Introduction

Lithium-ion batteries are the main driving force of most advances in electronic portable devices nowadays. Electrolytes for lithium-ion cells are dominated by LiPF₆ salt, which is almost exclusively used for electrolyte composing. Its advantages are high conductivity and wide electrochemical stability. Unfortunately, its disadvantages are numerous: hydrolysis with trace moisture [1], thermal stability as low as 68 °C [2] and low lithium cation transference number (T_{Li+}) [3]. Other notable salts are LiClO₄, known to be explosive [4], LiTf (lithium trifluoromethylsulfonate) and LiTFSI (lithium bis(trifluoromethylsulfonyl)imide) which are known to

cause aluminum corrosion [5]. Therefore, there is a persisting demand for lithium salt free of low T_{Li+} , thermal and electrochemical instability. That demand has enabled research oriented on multivalent salts in the past [6–8].

In large multivalent anion charge distribution is suggested to be more uniform. This phenomenon should effect T_{Li+} to be higher [6]. Unfortunately, all of multivalent salts' research have focused on sulfonyl imide derivatives [6–8] and as such are prone to sulfonyl imide disadvantages. The most important are expensive synthesis and low conductivity – in case of multivalent sulfonyl imide salts it is much smaller than this of LiTFSI. As for transference numbers, none have been measured for this class of salts. Also other alkali metal multivalent salts for electrochemical applications were based solely on this salt class [9].

Other related concepts include pseudo-localized zwitterion-type salts [10], also based on sulfonyl derivatives. These have not

* Corresponding author.

E-mail address: lniedzicki@ch.pw.edu.pl (L. Niedzicki).

yet been synthesized and as such, not investigated experimentally so far. Another idea of using polyanions as components of lithium-ion cell electrolytes has been investigated for some time [11,12]. Polyanions are known to have high T_{Li+} , but very low ionic conductivity – similar to traditional solid polymer electrolytes or even a lower one [13]. Also among polyanions the sulfonyl functional group has been playing a prominent role so far.

Recent success of imidazole-derived lithium salts [14–17], notably LiTDI (lithium 4,5-dicyano-2-(trifluoromethyl)imidazolate), has encouraged us to adapt this Hückel-class anion idea to tailor multivalent salt. As LiTDI exhibit high T_{Li+} itself, multivalent salt based on TDI structural fragment should exhibit even higher one. Also very high electrochemical and thermal stability of LiTDI should also be passed on to such a new anion.

Absence of oxygen atoms in this new salt should be an advantage due to lack of lithium favored coordination sites on oxygen atoms. That way lithium–anion interactions should be weakened and lithium cation transference number should increase. Aromatic rings presence, symmetrical geometry and numerous weak coordination sites for lithium should further increase T_{Li+} . Absence of hydrogen atoms should prohibit any proton-related issues such as increase of solution acidity or free acids forming. Trifluoromethyl electron-withdrawing groups in the anion should stabilize the charge (or charges) on the anion. Fluorine presence is known to increase compound stability against oxidation [18,19]. Proposed salt with such features – trilithium 2,2',2''-tris(trifluoromethyl)benzotris(imidazolate) (Li_3BTI) – is depicted in Fig. 1. In this paper we combine two novelties. First deals with the new path of systematic studies of imidazole Hückel anions. Secondly, here we present first multivalent lithium salt tailored specifically for lithium-ion cells which does not contain sulfonyl group.

2. Experimental methods

2.1. Synthesis of the Li_3BTI salt

An overview of the synthesis is depicted in Fig. 2. All commercially available chemicals were used as obtained.

Nuclear magnetic resonance (NMR) spectra were recorded on FT-NMR Bruker Avance 500 MHz with UltraShield 500 Plus 11.744 T superconducting magnet. Samples for NMR experiments were dissolved in deuterated dimethyl sulfoxide ($DMSO-d_6$, 99.96 atom % D, Aldrich).

Raman spectrum of pure crystalline salt was performed on Nicolet Almega dispersive spectrometer at room temperature. Diode laser with an excitation line at 780 nm was used. The spectral resolution was about 2 cm^{-1} .

2.1.1. 1,3,5-Trichloro-2,4,6-trinitrobenzene (2)

Potassium nitrate (121.2 g, 1.2 mol) was added to 25% oleum (496.8 mL, 960.12 g, 3 mol SO_3) at 65°C . The resulting mixture was then heated to 110°C and after becoming clear 1,3,5-trichlorobenzene **1** (27.21 g, 0.15 mol) was added with stirring.

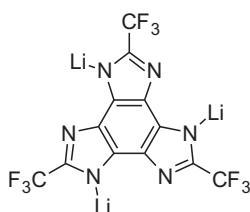


Fig. 1. Li_3BTI (trilithium 2,2',2''-tris(trifluoromethyl)benzotris(imidazolate)) salt.

The temperature was raised to 135°C and held for 12 h. After cooling to room temperature the viscous mixture was slowly poured onto flaked ice (2 kg). The solid which separated was filtered off, washed free of acid, dissolved in dichloromethane (300 mL) and dried with anhydrous Na_2SO_4 . After solvent evaporation and recrystallization of a crude product from methanol 1,3,5-tichloro-2,4,6-trinitrobenzene (33.69 g, 71%) was obtained as a pale yellow crystals (mp $192\text{--}195^\circ\text{C}$, lit. [20] mp 190°C from chloroform). ^{13}C NMR ($CDCl_3$, 125 MHz, δ): 122.3 (s, C–Cl, 3C), 147.4 (s, C– NO_2 , 3C).

2.1.2. 1,3,5-Triamino-2,4,6-trinitrobenzene (3)

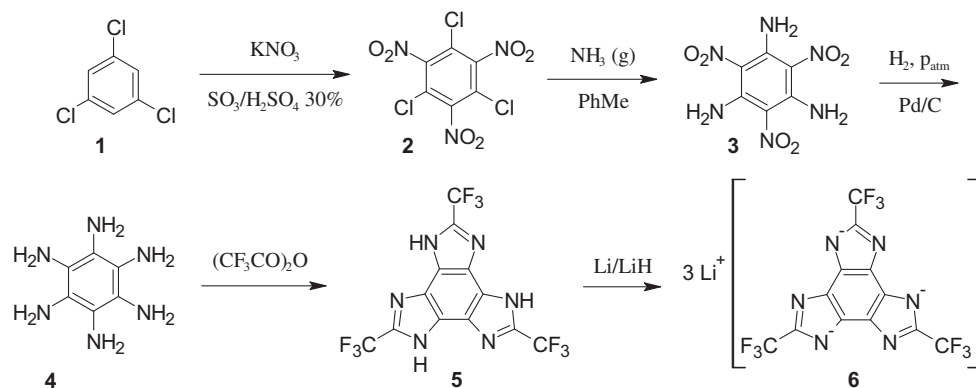
Through a boiling solution of 1,3,5-tichloro-2,4,6-trinitrobenzene **2** (49.6 g, 192 mmol) in toluene (1 L) an intensive flow of dry gaseous ammonia was passed. After 10 h resulting yellow suspension was cooled to room temperature and a precipitate was filtered off. The solid was washed with water until became free of chlorides, and then with methanol and dichloromethane. Drying on the air resulted 1,3,5-triamino-2,4,6-trinitrobenzene (18.9 g, 93%) as a yellow powder.

2.1.3. 2,2',2''-Tris(trifluoromethyl)benzotris(imidazole) (5)

1,3,5-Triamino-2,4,6-trinitrobenzene (5.0 g, 19.37 mmol) was suspended in ethyl acetate (230 mL) and hydrogenated with vigorous stirring at 60°C under normal pressure with 10% Pd/C (1.33 g) as catalyst. Hydrogen uptake stopped after 6 h when the suspension had become colorless. The solvent was evaporated with exclusion of oxygen (70°C , 15 Torr). 1,4-Dioxane (200 mL) was added to the residue and then trifluoroacetic anhydride (13.7 mL, 20.35 g, 96.85 mmol, 5 equiv) was added dropwise with vigorous stirring under argon atmosphere. The resulting solution was then refluxed (2 h) and after cooling to room temperature catalyst (Pd/C) was filtered off through diatomaceous earth layer. A filtrate was then transferred to a vessel equipped with a high-vacuum quality PTFE stopcock and concentrated hydrochloric acid (4 mL) was added. The reaction mixture was heated to $160\text{--}170^\circ\text{C}$ for 4 h. A crude product precipitated from the solution on cooling to room temperature overnight. The precipitate was filtered off, washed with water, dissolved in acetone and repeatedly evaporated with benzene in order to remove water. As a result 2,2',2''-tris(trifluoromethyl)benzotris(imidazole) (5.62 g, 72%) was obtained as a gray powder. ^{13}C NMR (125 MHz, $DMSO-d_6$, δ): 119.1 (q, $J = 270\text{ Hz}$, $-CF_3$, 3C), 124.6 and 126.6 (2s, C_{Ar} , $2 \times 3\text{C}$), 137.3 (q, $J = 40\text{ Hz}$, C– CF_3 , 3C). ^{19}F NMR (470 MHz, $DMSO-d_6$, δ): -44.3 (s).

2.1.4. Trilithium 2,2',2''-tris(trifluoromethyl)benzotris(imidazolate) (6) (short name Li_3BTI)

To a solution of 2,2',2''-tris(trifluoromethyl)benzotris(imidazole) (3.0 g, 7.46 mmol) in anhydrous THF (50 mL) metallic lithium pellets (0.30 g, 43.23 mmol, 5.8 equiv) were added under argon atmosphere. After 24 h the excess of lithium was removed by filtration and solution was evaporated. The residue was chromatographed (aluminum oxide neutral, 50 g, eluted with anhydrous acetonitrile, 250 mL). Combined fractions containing white monolithium salt were evaporated and dissolved in THF (50 mL). Then lithium hydride (130 mg, 16.41 mmol, 2.2 equiv) was added. After hydrogen evolution stopped reaction mixture was filtered and a filtrate was evaporated giving trilithium 2,2',2''-tris(trifluoromethyl)benzotris(imidazolate) (2.5 g; 80%) as a pale yellow powder. ^{13}C NMR (125 MHz, $DMSO-d_6$, δ): 121.8 (q, $J = 672\text{ Hz}$, $-CF_3$, 3C), 129.6 (s, C_{Ar} , 6C), 139.6 (q, $J = 91\text{ Hz}$, C– CF_3 , 3C). ^{19}F NMR (470 MHz, $DMSO-d_6$, δ): -61.9 (s). Raman (780 nm, cm^{-1}): 1649, 1559, 1536, 1399, 1315, 1295, 1228, 1067, 983, 917, 898, 767, 607, 449, 443, 331, 229.

Fig. 2. Synthesis of Li₃BTI.

2.2. Measurement techniques

TGA and DSC were performed on Du Pont Thermal Analyst System 2100. Measurements were made in open ceramic pans in air atmosphere in 30–450 °C. Heating rate was equal to 10 K min^{−1}.

All samples for measurements were assembled in argon-filled drybox with moisture level less than 1 ppm. Prior to assembly, the salt was vacuum-dried for 48 h in 80 °C. Solvents (propylene carbonate (PC), ethylene carbonate (EC), dimethyl carbonate (DMC)) were anhydrous and used as provided (water content <20 ppm for PC and DMC, <50 ppm for EC).

Linear Sweep Voltammetry (LSV), conductivity measurements and lithium cation transference number (T_{Li^+}) were performed on VMP3 (Bio-Logic Science Instruments) multichannel potentiostat with Frequency Response Analyzer.

For LSV measurements samples were assembled in Li|electrolyte|Pt system and the scan rate was 10 mV s^{−1}. Measurements were performed at room temperature. Lithium metal was used for both reference and counter electrode.

Ionic conductivity measurements used Electrochemical Impedance Spectroscopy (EIS) technique for obtaining resistance. Samples were thermostated for at least 1 h at each temperature in Haake D50 cryostat in 0–50 °C temperature range with 10 °C interval with 0.05 °C precision. Prior to experiments cell constants were calibrated with KCl solutions with at least 0.3% precision.

T_{Li^+} experiments used Li|electrolyte|Li cells and were performed at room temperature. T_{Li^+} was determined using standard Bruce-Vincent-Evans method [21] using a following equation: $T_+ = (I_s (\Delta V - I_0 R_0)) / (I_0 (\Delta V - I_s R_s))$, where ΔV was a polarization voltage equal to 20 mV; I_0 and I_s were initial and steady-state current during said polarization, respectively; R_0 and R_s were resistances of solid electrolyte interface (SEI) immediately before and after polarization, respectively. EIS was performed in 500 kHz–100 mHz frequency range with 5 mV ac amplitude. At least 3 samples were measured for each electrolyte composition to ensure data consistency. Standard deviation was not higher than 0.03 for any electrolyte. Detailed description of this method can be found in other papers [16].

Charge–discharge cycling used Li | electrolyte | LiCoO₂ or Li|electrolyte|Si–C half-cell system with silicon–carbon nanostructured composite thin-film anode obtained through use of microwave plasma assisted chemical vapor deposition (MPCVD). Triethoxy(octyl)silane was used here as precursor. Details of the MPCVD method for nano-structured composite electrodes manufacturing are described elsewhere [22]. Cycling voltage was set in 2.7–3.2 V range (half-cell containing LiCoO₂) or 0.05–1.4 V (half-cell containing Si–C) range. Current was chosen every time in such a way that both discharge and charge would take 1 h (1 C

current). Electrolytes used were as follows: 0.25 M Li₃BTI in pure PC and 0.25 M Li₃BTI in EC:DMC (1:1 weight ratio). Astrol Electronic Bat-Small battery cycler was used for cycling experiment.

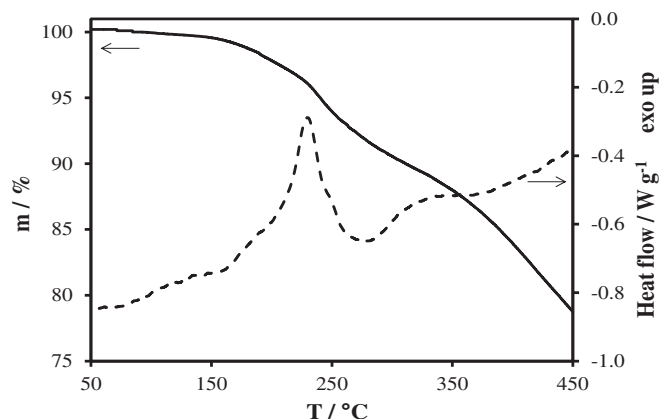
3. Results and discussion

Li₃BTI thermal stability measurement results are shown on Fig. 3. Thermal decomposition onset is visible at 160 °C. It is definitely lower than thermal decomposition of its monovalent analog LiTDI (257 °C). On the other hand it exceeds some monovalent commercially available salts [2]. Also, thermal stability of Li₃BTI is higher than most battery solvent boiling points (DMC, DEC, EMC) [23], so it is not a limiting factor for lithium-ion cell safety.

Electrochemical stability window is depicted on Fig. 4. There is lack of any LSV signals within 0.1–4.2 V vs Li range. Anodic decomposition onset is visible at 4.2 V vs Li.

Fig. 5 depicts conductivity of Li₃BTI solutions in PC. A wide range of concentration have been investigated. Maximum solubility of Li₃BTI was just above 0.75 M. A monotonic dependence between concentration and conductivity can be observed. One exception form such a monotonic dependence can be indicated: 0.25 M concentration at higher temperatures. This composition exhibits higher conductivity energy activation. Hence its conductivity increase with temperature is faster than that of other concentrations.

Ionic conductivity of 0.75 M Li₃BTI-PC electrolyte at 20 °C is equal to 0.43 mS cm^{−1}. It is worth noting that ionic conductivity is decreasing very slowly with concentration. 0.1 M Li₃BTI-PC solution at 20 °C reach value of 0.31 mS cm^{−1}. Conductivity of 0.1 mS cm^{−1} at room temperature is obtained at concentration as low as 0.01 M.

Fig. 3. Thermal stability of Li₃BTI, studied with TGA (solid line) and DSC (dashed line).

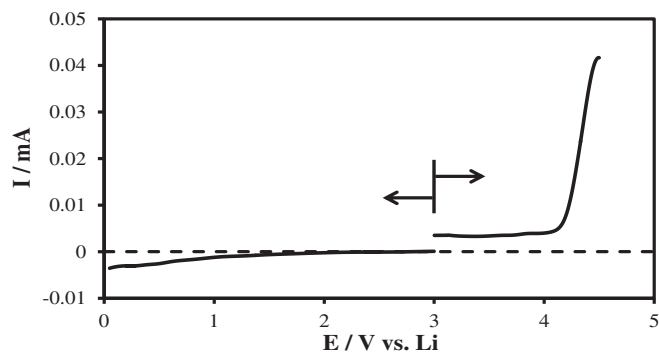


Fig. 4. Linear sweep voltammetry plots of 0.1 M Li_3BTI solution in propylene carbonate on platinum electrode.

Li_3BTI conductivity in EC:DMC (1:1 weight ratio) battery mixture-type solutions is shown on Fig. 6. Simple conductivity dependence of concentration can be observed. Maximum solubility in this solvent mixture is the same as in case of PC solutions (0.75 M). Conductivity of solutions in this solvent mixture is visibly higher than for PC-based electrolytes. Ionic conductivity at 20 °C is highest for the 0.75 M Li_3BTI -EC:DMC electrolyte and is equal to 0.85 mS cm^{-1} .

Lithium cation transference number measurement results for Li_3BTI -PC and Li_3BTI -EC:DMC electrolytes in full range of concentrations are shown on Fig. 7. As predicted at the concept phase, the T_{Li^+} values are extraordinarily high. In case of 0.75 M Li_3BTI in EC:DMC solution it is as high as 0.73. All other EC:DMC solutions of this multivalent salt, T_{Li^+} values exceed 0.65.

In case of Li_3BTI -PC solutions lithium cation transference number parameter has maximum at 0.25 M concentration, at which it equals 0.72. Towards higher concentration, T_{Li^+} decrease slowly to reach 0.67 at 0.75 M concentration. As for solutions more dilute than 0.25 M concentration, high T_{Li^+} value is maintained down to 0.05 M Li_3BTI -PC, at which it reach value of 0.63. At lowest investigated concentrations T_{Li^+} value drop to 0.47 in case of 0.01 M Li_3BTI -PC solution. It is worth stressing that 0.25 M concentration lithium cation transference number maximum is overlapping with unusually high conductivity activation energy. In case of this solution ionic conductivity at high temperatures (over 40 °C) is higher than for 0.5 M solution. That indicates change of predominant conducting species (associate)

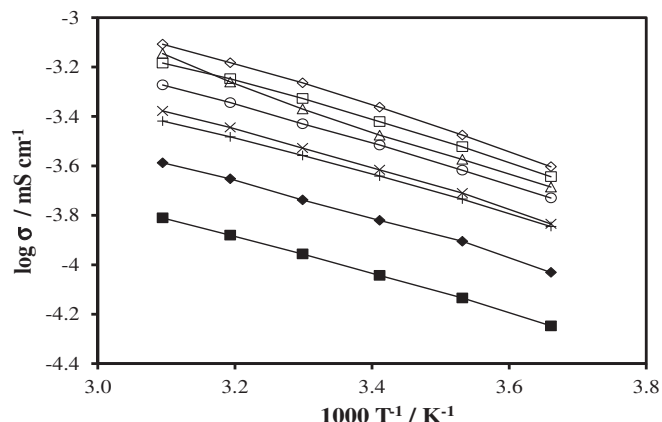


Fig. 5. Conductivity dependence of Li_3BTI concentration in propylene carbonate in the 0–50 °C range. Following concentrations are shown on the figure: 0.75 M (◇), 0.5 M (□), 0.25 M (△), 0.1 M (×), 0.05 M (+), 0.025 M (◆), 0.01 M (■). Lines are only to guide the eye.

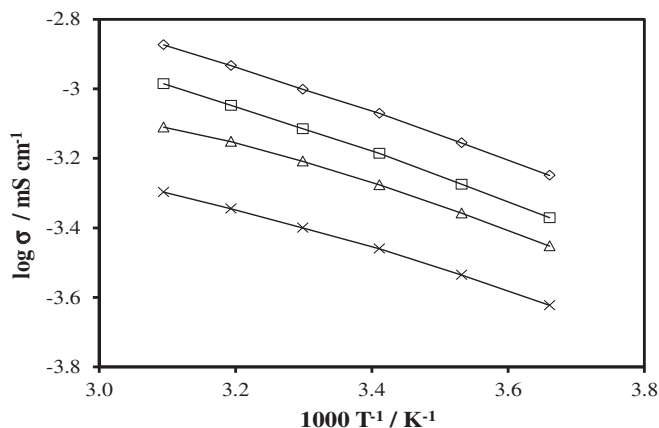


Fig. 6. Conductivity dependence of Li_3BTI concentration in mixture of ethylene carbonate and dimethyl carbonate (1:1 weight ratio) in the 0–50 °C range. Following concentrations are shown on the figure: 0.75 M (◇), 0.5 M (□), 0.25 M (△), 0.1 M (×). Lines are only to guide the eye.

at this concentration. Nevertheless, it is quite beneficial for the electrolyte parameters.

Molar conductivity of Li_3BTI in PC and lithium cation transference number are plotted against square root of concentration on Fig. 8. Molar conductivity is decreasing with the concentration growth. Minor deviation from the trend is visible in both plots at 0.1 mol dm^{-3} . Presence of such deviation could suggest formation of the new ionic agglomerate in the investigated concentration range. More significant trend changes are visible in the molar conductivity plots of LiTDI in PC (LiTDI is the most similar imidazole-derivative salt to Li_3BTI , data not shown here, reported by us elsewhere) [16]. However, all plot changes in Li_3BTI case may be less apparent due to the bigger number of ions (stoichiometrically) and more possible combinations of them in the solution. Existence of such fluctuation (like the one observed at 0.1 mol dm^{-3}) may imply a quality change in ionic association in the solution at this concentration. Positive deviation in case of molar conductivity at such high concentration may suggest formation of new charged associate(s). Local decrease of cation transference number could mean formation of negative-charged associate or addition of lithium cation to agglomerate in which lithium is already present. Due to the much higher concentration of free lithium cations than BTI anions in the solution (3:1 ratio and high negative charge of the solitary anion), the latter is much more likely. One can only assume that due to overlap of minor local

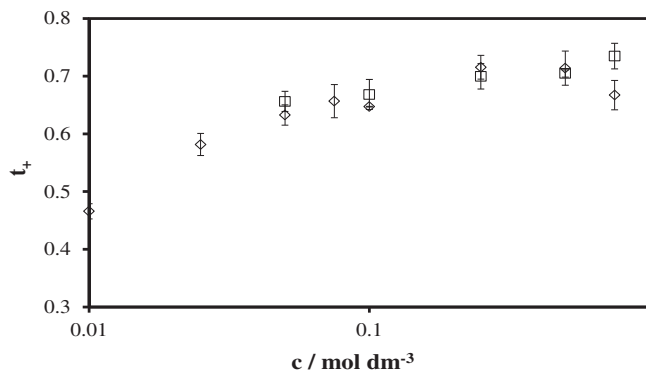


Fig. 7. Lithium cation transference number dependence of Li_3BTI concentration in propylene carbonate (◇) and in mixture of ethylene carbonate and dimethyl carbonate, 1:1 weight ratio (□).

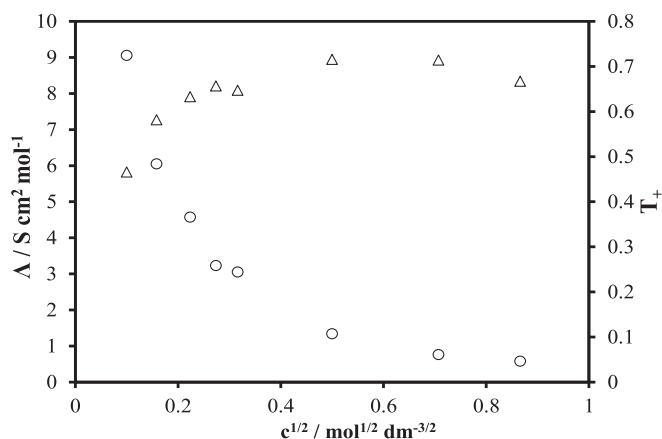


Fig. 8. Molar conductivity (\circ , left y-axis) and lithium cation transference number (Δ , right y-axis) dependence of Li_3BTI square root of concentration in propylene carbonate at 20°C .

decrease of lithium cation transference number and local positive deviation of molar conductivity, such agglomerate is forming through a lithium cation addition to neutral associate like Li_3BTI , e.g. Li_4BTI^+ .

Fig. 9 depicts results of galvanostatic cycling of half-cells containing Li_3BTI solutions as electrolytes against Si/C electrodes. This is the final proof of concept of both salt stability and applicability in lithium-ion cells. In case of Li_3BTI -PC electrolyte reversible discharge capacity is as high as 612 mAh g^{-1} . However, electrode gradual capacity fading ($\sim 23\%$) over time is noticed. Such capacity decrease can be attributed to electrode electrolyte interactions. Propylene carbonate is known to exfoliate graphite layers, which effects in electrode degradation [23,24]. To prove that this is the case and Li_3BTI is stable when cycled, additional cycling with EC:DMC solution has been conducted. This time the initial discharge capacity was lower (379 mAh g^{-1}), but almost no electrode degradation has been observed. Over 50 cycles discharge capacity changed by only 7%, without use of any stabilizing additives.

Fig. 10 shows preliminary results of additional galvanostatic cycling of half-cells containing Li_3BTI solutions as electrolytes against LiCoO_2 electrodes. Degradation (40% over 20 cycles) of electrode during cycling with EC:DMC solution is visible. No such negative effect is observed during cycling with PC solution (only 3% capacity decrease over 20 cycles). Although purely preliminary, such results prove salt stability against both low and high potentials in the cell.

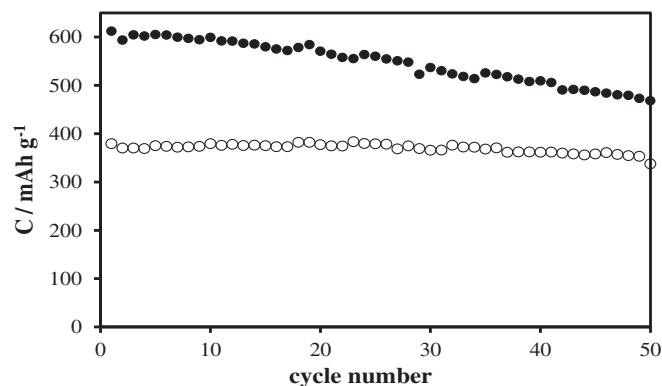


Fig. 9. Discharge capacity of $\text{Li}|\text{0.25 M Li}_3\text{BTI}$ in PC (\bullet) (or EC:DMC (\circ))|Si-C at 1 C rate charge–discharge cycling in $0.05\text{--}1.40\text{ V}$ vs Li/Li^+ range.

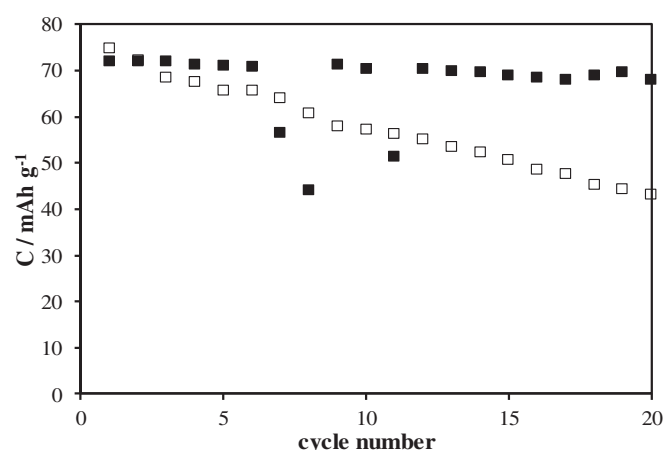


Fig. 10. Discharge capacity of $\text{Li}|\text{0.25 M Li}_3\text{BTI}$ in PC (\blacksquare) (or EC:DMC (\square))| LiCoO_2 at 1 C rate charge–discharge cycling in $2.7\text{--}3.2\text{ V}$ vs Li/Li^+ range.

4. Conclusions

Novel multivalent lithium salt has been proposed and synthesized especially for lithium-ion cells. Synthesis route was chosen in such a way to be easy, three-step and use inexpensive substrates. Trilithium 2,2',2''-tris(trifluoromethyl)benzotris(imidazolate) – Li_3BTI – has been designed to reach exceptionally high lithium cation transference number, without sacrificing salt stability. In fact, t_{Li^+} values of Li_3BTI (higher than 0.7 in both tested solvents) are considerably higher than those of any other lithium-ion cell applicable lithium salt. However, the electrochemical (up to 4.2 V vs Li) or thermal (160°C) stability is not compromised. Ionic conductivity is reaching 1 mS cm^{-1} order of magnitude at room temperature. Cycling in half-cells proved that salt can be safely used in lithium-ion cell electrolyte and form stable solid–electrolyte interface. Thus, we have obtained the proof of concept for multivalent anion with uniform charge distribution.

Acknowledgments

This work has been supported by the Ventures grant of the Foundation for Polish Science, contract no. VENTURES/2012-9/8, funded by the European Regional Development Fund and the Innovative Economy Operational Programme.

This work has been supported by the European Union in the framework of European Social Fund through the Warsaw University of Technology Development Programme, realized by Center for Advanced Studies.

This work has been financially supported by Warsaw University of Technology.

References

- [1] X.-G. Teng, F.-Q. Li, P.-H. Ma, Q.-D. Ren, S.-Y. Li, *Thermochim. Acta* 436 (2005) 30.
- [2] Z. Lu, L. Yang, Y. Guo, *J. Power Sources* 156 (2006) 555.
- [3] M. Riley, P.S. Fedkiw, S.A. Khan, *J. Electrochem. Soc.* 149 (2002) A667.
- [4] R. Jasinski, S. Carroll, *J. Electrochem. Soc.* 117 (1970) 218.
- [5] L.J. Krause, W. Lamanna, J. Summerfield, M. Engle, G. Korba, R. Loch, R. Atanasoski, *J. Power Sources* 60 (1997) 320.
- [6] O.E. Geiculescu, J. Yang, H. Blau, R. Bailey-Walsh, S.E. Creager, W.T. Pennington, D.D. DesMarteau, *Solid State Ionics* 148 (2002) 173.
- [7] O.E. Geiculescu, Y. Xie, R. Rajagopal, S.E. Creager, D.D. DesMarteau, *J. Fluorine Chem.* 125 (2004) 1179.
- [8] R.Y. Garlyauskayte, A.N. Chernega, C. Michot, M. Armand, Y.L. Yagupolskii, L.M. Yagupolskii, *Org. Biomol. Chem.* 3 (2005) 2239.
- [9] J. Nie, X. Li, D. Liu, R. Luo, L. Wang, *J. Fluorine Chem.* 125 (2004) 27.
- [10] E. Jonsson, M. Armand, P. Johansson, *Phys. Chem. Chem. Phys.* 14 (2012) 6021.

- [11] M. Watanabe, H. Tokuda, S. Muto, *Electrochim. Acta* 46 (2001) 1487.
- [12] R. Meziane, J.-P. Bonnet, M. Courty, K. Djellab, M. Armand, *Electrochim. Acta* 57 (2011) 14.
- [13] S. Feng, D. Shi, F. Liu, L. Zheng, J. Nie, W. Feng, X. Huang, M. Armand, Z. Zhou, *Electrochim. Acta* 93 (2013) 254.
- [14] L. Niedzicki, M. Kasprzyk, K. Kuziak, G.Z. Zukowska, M. Armand, M. Bukowska, M. Marcinek, P. Szczeciński, W. Wieczorek, *J. Power Sources* 192 (2009) 612.
- [15] L. Niedzicki, G.Z. Zukowska, M. Bukowska, P. Szczeciński, S. Grugeon, S. Laruelle, M. Armand, S. Panero, B. Scrosati, M. Marcinek, W. Wieczorek, *Electrochim. Acta* 55 (2010) 1450.
- [16] L. Niedzicki, M. Kasprzyk, K. Kuziak, G.Z. Zukowska, M. Marcinek, W. Wieczorek, M. Armand, *J. Power Sources* 196 (2011) 1386.
- [17] L. Niedzicki, S. Grugeon, S. Laruelle, P. Judeinstein, M. Bukowska, J. Prejzner, P. Szczeciński, W. Wieczorek, M. Armand, *J. Power Sources* 196 (2011) 8696.
- [18] T. Achiha, T. Nakajima, Y. Ohzawa, M. Koh, A. Yamauchi, M. Kagawa, H. Aoyama, *J. Electrochem. Soc.* 156 (2009) A483.
- [19] T. Achiha, T. Nakajima, Y. Ohzawa, M. Koh, A. Yamauchi, M. Kagawa, H. Aoyama, *J. Electrochem. Soc.* 157 (2010) A707.
- [20] M.E. Hill, F. Taylor Jr., *J. Org. Chem.* 25 (1960) 1037.
- [21] P.G. Bruce, C.A. Vincent, *J. Electroanal. Chem.* 225 (1987) 1.
- [22] M. Marcinek, L.J. Hardwick, T.J. Richardson, X. Song, R. Kostecki, *J. Power Sources* 173 (2007) 965.
- [23] K. Xu, *Chem. Rev.* 104 (2004) 4303.
- [24] A.N. Dey, B.P. Sullivan, *J. Electrochem. Soc.* 117 (1970) 222.